*J. Fluid Mech.* (1972), *vol.* 54, *part* 2, *pp.* 305–337
*Printed in Great Britain*



# Three-dimensional wings in hypersonic flow

By R. HILLIER
Engineering Department, Cambridge University†

(Received 24 March 1972)

Messiter's thin shock layer approximation for hypersonic wings is applied to several non-conical shapes. Two calculation methods are considered. One gives the exact solution for a particular three-dimensional geometry which possesses a conical planform and also a conical distribution of thickness superimposed upon a surface cambered in the chordwise direction. Agreement with experiment is good for all cases, including that where the wing is yawed. The other method is a more general approach whereby the solution is expressed as a correction to an already known conical flow. Such a technique is applicable to conical planforms with either attached or detached shocks but only to the non-conical planform for the region in the vicinity of the leading edge when the shock is attached.

## 1. Introduction

In recent years there has been considerable interest in predicting the flow around lifting bodies at high supersonic or hypersonic speeds and in consequence a variety of calculation methods have been developed. These have generally been discussed in detail in the literature (see, for example, Hayes & Probstein (1966) and also *Analytical Methods in Aircraft Design*, N.A.S.A. SP-228) and the purpose of this paper is to present further developments of one particular theory, the so-called thin shock layer approximation.

This theory studies the case where the shock lies very close to the body surface; under such conditions the flow variables in the intervening shock layer may be written as series expansions in terms of some appropriate hypersonic parameter or parameters which, in their turn, are a measure of the thinness of the layer. The zeroth-order terms of these series then give the well-known basic Newtonian results, modified possibly by the Busemann correction for body curvature. The theory has been extensively applied to the blunt body case and, again, this is reviewed by Hayes & Probstein. The earliest applications of direct relevance to hypersonic wings were those due to Cole & Brainerd (1962) and also to Antonov & Hayes (1966), who effectively studied the problem of slender wings at very high incidences. The flow in the cross-plane is the dominant factor in this case and chordwise variations are neglected. Generally such variations are important, however, and this case was originally studied by Messiter (1963), who derived a set of approximate equations of motion subject to certain limitations on the body geometry. First, it must correspond to that of what Hayes & Probstein term a blunt-faced body, i.e. a nearly planar compression surface generating the shock

† Present address: Central Electricity Research Laboratories, Leatherhead, Surrey.

such that one angle of attack typifies the incidence of every element of the body surface. Second, only the flow over the compression suface can be considered by the theory. This side is separated by the trace of a sharp leading edge from the suction surface, which is itself assumed to be at vacuum conditions or, rather, it is assumed that the pressure is sufficiently low not to interfere with the flow over the compression side. The wing has a sharp vertex, at which the shock is attached, although it may be either attached or detached along the leading edges. It is this second condition, and not that at the vertex, which is implied by the terms attached or detached shocks in this work.

Only one hypersonic or perturbation parameter is required in Messiter's formulation. This is $\epsilon$, a quantity defining the density ratio across a plane shock lying at the same incidence $\alpha$ as the wing. Messiter specialized the approximate equations to the conical case and produced limited results for the lifting flat delta wing with a detached shock. This work was then followed by that of Hida (1965), who made an approximate allowance for wing thickness, and also of Squire (1966, 1968*a*), who obtained exact numerical solutions to the governing equations for the flow, with detached shocks, over conical wings with flat, diamond and caret (inverted 'V') cross-sections to the compression surfaces. These all showed excellent agreement with experiment, as did also the work by Hillier (1970*a*, *b*), who extended the analysis to include the effects of yaw upon wings with flat, convex and concave compression surfaces. In four further papers Squire (1968*b*), Woods (1970) and Roe (1970, 1971) all considered conical flows for the attached shock case, again showing good agreement with the limited experimental results and exact solutions available.

The main feature of the conical problem is that the perturbation $w$ in the cross-flow velocity (from the basic Newtonian value) is constant on a conical stream surface $\eta$ (say) and that the function $w(\eta)$ is itself related to the body geometry by a complicated integral equation. The above papers were all essentially concerned with the solution of this equation. Once $w(\eta)$ is known the evaluation of the other flow properties is straightforward although complicated algebraically.

The purpose of the present work is to present some extensions of the theory to non-conical wings; however, since the analysis depends to a large extent upon results derived for the conical case, and since the reader may not be fully acquainted with these, the relevant work is reviewed in the earlier parts of the text. The full analysis may therefore be followed without recourse to the quoted literature, apart from the more detailed points.

Two main classes of wing become apparent in the three-dimensional analysis, depending upon whether the wing planform is conical or not, but with no apparent limitation upon the actual form of the thickness distribution. The non-conical planform has not proved readily amenable to analysis and, as yet, the method only holds for the region in the vicinity of a curved leading edge with an attached shock. However, the conical planform is not limited to the attached shock case and several important results have been derived. The first is an exact solution for the simply cambered bodies, defined as those possessing a conical distribution of thickness superimposed upon a surface cambered in the chordwise direction. This result includes the effects of yaw and shows good agreement with experiment.

No exact solution has been derived for any other three-dimensional body but such cases may be studied by a perturbation technique whereby the flow variables are expanded further as a series in $x$, the chordwise distance from the vertex. The solution at the vertex, i.e. the first term of the series, is then a conical result, which is assumed to be already known. Each higher correction depends upon the appropriate perturbation in the cross-flow velocity and this, in turn, is related to the perturbation in the body geometry by an integral equation, similar to the one obtained for the conical case itself. Only the analysis for the first correction is given in full since it in fact typifies the technique for all higher corrections. Agreement with experiment is variable for this approach. The centre-line pressure on the unyawed wing, which is in fact given exactly by the theory, and also the pressure at the leading edge for an attached shock compare well. However, the calculated pressure on the outer half of the wing span, for the one available comparison with a detached shock case, shows disappointing agreement in view of the generally excellent results expected from the earlier work for the conical case.

## 2. Derivation of the thin shock layer equations

The thin shock layer equations have been presented in several of the references. However, the full three-dimensional equations for a yawed wing are rederived here for completeness since they serve as a useful introduction to the present work and also constitute the basis of any attempt to calculate higher order corrections.

Figure 1 shows a uniform supersonic stream with speed $\overline{U}_\infty$ and Mach number $M_\infty$ impinging upon a wing of arbitrary shape at an angle of incidence $\alpha$ and an angle of yaw $\beta$. The vertex of the wing is at the origin, i.e. at $\bar{x} = \bar{y} = \bar{z} = 0$, and the plane $\bar{y} = 0$ is coincident with the plane of the wing's leading edges at the vertex. The angle of incidence $\alpha$ is also measured with respect to this plane as indicated in the figure.

The purpose of this section is to derive a consistent system of approximate equations of motion and boundary conditions from the exact equations of fluid motion; these give the following equations for the steady flow of an ideal inviscid gas.

Continuity: $$\nabla.(\bar{\rho}\bar{\mathbf{q}}) = 0. \tag{2.1}$$

Momentum: $$\bar{\mathbf{q}}.\nabla\bar{\mathbf{q}} + (1/\bar{\rho})\nabla\bar{p} = 0. \tag{2.2}$$

Entropy: $$\bar{\mathbf{q}}.\nabla(\bar{p}/\bar{\rho}^\gamma) = 0. \tag{2.3}$$

The overbar indicates quantities evaluated in the physical plane, as opposed to the transformed planes which will be used later. The above equations must be evaluated subject both to the body surface boundary conditions and also to the Rankine–Hugoniot conditions at the shock. The first requires that streamlines eventually become tangential to the body surface and is expressed by

$$\bar{\mathbf{q}}_B.\bar{\mathbf{n}}_B = 0 \quad \text{on} \quad \bar{y} = \bar{y}_B, \tag{2.4}$$

where $\bar{\mathbf{n}}_B$ is the unit vector normal to the body and $\bar{\mathbf{q}}_B$ is the velocity vector evaluated on the surface; the subscript $B$ refers to the body surface.

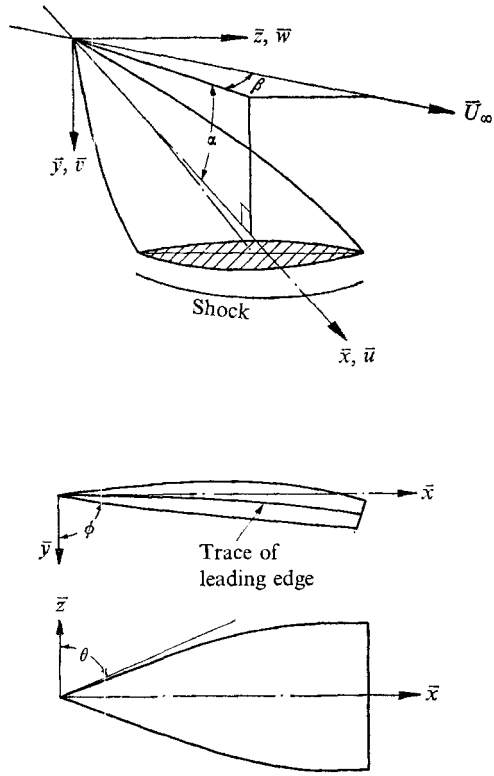


FIGURE 1. Nomenclature for yawed wing ($b = \cot\theta$, $h = \cot\phi$).

The jump conditions at the shock give the following conditions.

Continuity: $$[\bar{\rho}(\bar{\mathbf{q}}.\bar{\mathbf{n}}_s)] = 0. \tag{2.5}$$

Momentum: $$[\bar{p}+\bar{\rho}(\bar{\mathbf{q}}.\bar{\mathbf{n}}_s)^2] = 0. \tag{2.6}$$

Energy: $$[\tfrac{1}{2}(\bar{\mathbf{q}}.\bar{\mathbf{n}}_s)^2+\{\gamma/(\gamma-1)\}\bar{p}/\bar{\rho}] = 0. \tag{2.7}$$

Tangential velocity: $$[\bar{\mathbf{q}}\times\bar{\mathbf{n}}_s] = 0. \tag{2.8}$$

Here the square brackets denote the change in the enclosed quantity across the shock discontinuity and $\bar{\mathbf{n}}_s$ is the unit vector normal to the shock surface and is directed away from the body. If the shock shape $\bar{y}_s(\bar{x},\bar{z})$ is represented by

$$\bar{S}(\bar{x},\bar{y},\bar{z}) = \bar{y}-\bar{y}_s(\bar{x},\bar{z}) = 0 \tag{2.9}$$

then the unit vector $\bar{\mathbf{n}}_s$ is

$$\bar{\mathbf{n}}_s = \frac{\nabla\bar{S}}{|\nabla\bar{S}|} = \frac{-\mathbf{i}\,\partial\bar{y}_s/\partial\bar{x}+\mathbf{j}-\mathbf{k}\,\partial\bar{y}_s/\partial\bar{z}}{[1+(\partial\bar{y}_s/\partial\bar{x})^2+(\partial\bar{y}_s/\partial\bar{z})^2]^{\frac{1}{2}}}. \tag{2.10}$$

Equations (2.5)–(2.10) are sufficient to determine all the shock properties in terms of the upstream flow conditions and the, as yet unknown, shock geometry. Messiter used this to assess the orders of magnitude of the flow properties in the shock layer for a nearly plane shock lying close to the blunt-faced body surface. The algebra for this is lengthy, and cannot be fully repeated here, but is given in more detail in Messiter (1963) and Hillier (1970*b*). Messiter proposed that the

true hypersonic limit $\gamma \to 1$, $M_\infty \sin\alpha \to \infty$ should be replaced by the condition $\epsilon \to 0$, where

$$\epsilon = \frac{\gamma-1}{\gamma+1} + \frac{2}{(\gamma+1)}\frac{1}{M_\infty^2 \sin^2\alpha \cos^2\beta}$$

is the density ratio across a basic two-dimensional shock lying in the plane $\bar{y} = 0$. He further proposed that in this hypersonic limit the various co-ordinates all scale in such a manner that the new stretched co-ordinates all remain of order unity as the shock layer thickness becomes vanishingly small. The resulting scalings, which are expected to hold at least in the outer part of the shock layer, then give

$$x^* = \bar{x}/\bar{c}, \tag{2.11}$$

$$y^* = \bar{y}/\bar{c}\,\epsilon \tan\alpha, \tag{2.12}$$

$$z^* = \bar{z}/\bar{c}\,\epsilon^{\frac{1}{2}} \tan\alpha, \tag{2.13}$$

where the $y^*$ scaling results from arguments concerning the continuity of streamwise flow (see, also, Roe 1970) and the $z^*$ scaling ensures that the Mach angle of the flow in the shock layer ($\epsilon^{\frac{1}{2}} \tan\alpha$ for $\epsilon \to 0$) is of the same order as the sweep angle $\theta$; this latter condition is important and makes certain that the approximation covers the cases of both attached and detached shocks. Thus, (2.13) also defines an appropriate sweepback parameter $\Omega$ (say) given by

$$\Omega = \cot\theta/\epsilon^{\frac{1}{2}} \tan\alpha. \tag{2.14}$$

The projection of the angle of yaw $\beta$ upon the plane $\bar{y} = 0$ scales in a similar manner to give the parameter for yaw, $\tau$ (say):

$$\tau = \tan\beta/\epsilon^{\frac{1}{2}} \sin\alpha. \tag{2.15}$$

After slightly modifying Messiter's arguments to include the effects of yaw, the flow variables in the shock layer are expanded in terms of $\epsilon$ to give

$$\bar{u}(\bar{x},\bar{y},\bar{z})/\bar{U}_\infty = \cos\alpha\cos\beta + (\epsilon \sin^2\alpha \cos\beta/\cos\alpha)\, u^*(x^*,y^*,z^*) + O(\epsilon^2), \tag{2.16}$$

$$\bar{v}(\bar{x},\bar{y},\bar{z})/\bar{U}_\infty = \epsilon \sin\alpha \cos\beta \times v^*(x^*,y^*,z^*) + O(\epsilon^2), \tag{2.17}$$

$$\bar{w}(\bar{x},\bar{y},\bar{z})/\bar{U}_\infty = \epsilon^{\frac{1}{2}} \sin\beta \cos\alpha \times w^*(x^*,y^*,z^*) + O(\epsilon^{\frac{3}{2}}), \tag{2.18}$$

$$(\bar{p}-\bar{p}_\infty)/\tfrac{1}{2}\bar{\rho}_\infty \bar{U}_\infty^2 = C_p = 2\sin^2\alpha \cos^2\beta[1 + \epsilon p^*(x^*,y^*,z^*)] + O(\epsilon^2), \tag{2.19}$$

$$\bar{\rho}_\infty/\bar{\rho} = \epsilon + \epsilon^2 \sigma^*(x^*,y^*,z^*) + O(\epsilon^3), \tag{2.20}$$

where the zeroth-order term in each case is the appropriate basic Newtonian value. Evaluation of the shock boundary conditions (2.5)–(2.8) gives

$$u_s^* = -\partial y_s^*/\partial x^*, \tag{2.21}$$

$$v_s^* = -1 + \frac{\partial y_s^*}{\partial x^*} - \left(\frac{\partial y_s^*}{\partial z^*}\right)^2 + \tau \frac{\partial y_s^*}{\partial z^*} \tag{2.22}$$

$$w_s^* = \tau - \partial y_s^*/\partial z^*, \tag{2.23}$$

$$p_s^* = -1 + 2\frac{\partial y_s^*}{\partial x^*} - \left(\frac{\partial y_s^*}{\partial z^*}\right)^2 + 2\tau \frac{\partial y_s^*}{\partial z^*}, \tag{2.24}$$

$$\sigma_s^* = \frac{2}{N}\left\{-2\frac{\partial y_s^*}{\partial x^*} + 2\tau \frac{\partial y_s^*}{\partial z^*} + \left(\frac{\partial y_s^*}{\partial z^*}\right)^2\right\}, \tag{2.25}$$

where

$$N = 2 + (\gamma-1) M_\infty^2 \sin^2\alpha \cos^2\beta. \tag{2.26}$$

The thin shock layer equations are now derived by substituting (2.16)–(2.20) into the full equations of motion (2.1)–(2.3) and retaining only the lowest terms in $\epsilon$. This gives

$$\frac{\partial v^*}{\partial y^*}+\frac{\partial w^*}{\partial z^*}=0, \tag{2.27}$$

$$\frac{\partial u^*}{\partial x^*}+v^*\frac{\partial u^*}{\partial y^*}+w^*\frac{\partial u^*}{\partial z^*}=0, \tag{2.28}$$

$$\frac{\partial v^*}{\partial x^*}+v^*\frac{\partial v^*}{\partial y^*}+w^*\frac{\partial v^*}{\partial z^*}=-\frac{\partial p^*}{\partial y^*}, \tag{2.29}$$

$$\frac{\partial w^*}{\partial x^*}+v^*\frac{\partial w^*}{\partial y^*}+w^*\frac{\partial w^*}{\partial z^*}=0, \tag{2.30}$$

$$\sigma^*=-(1+p^*)-\frac{(N-2)}{N}(2u^*+w^{*2}), \tag{2.31}$$

where (2.27) is the new reduced form for the continuity equation and (2.28)–(2.30) are the $\bar{x}$, $\bar{y}$ and $\bar{z}$ momentum equations respectively and $\sigma^*$, the perturbation in density, is related to the other flow properties by the energy equation for isentropic flow. Equations (2.27)–(2.31) must be solved subject to both the shock boundary conditions (2.21)–(2.25) and also the body surface tangency condition. This latter condition is expressed by (2.4) and reduces in the thin shock layer limit to

$$-\frac{\partial y_B^*}{\partial x^*}+v^*-w^*\frac{\partial y_B^*}{\partial z^*}=0 \quad \text{on} \quad y^*=y_B^*. \tag{2.32}$$

## 3. Discussion of the thin shock layer equations

Before progressing further with the analysis the main points of the above equations will be discussed. In the thin shock layer theory the total derivative along a streamline is given by

$$\frac{\partial}{\partial x^*}+v^*\frac{\partial}{\partial y^*}+w^*\frac{\partial}{\partial z^*}, \tag{3.1}$$

so (2.28) and (2.30) show that both $u^*$ and $w^*$ remain constant for a fluid particle as it progresses through the shock layer; thus a streamline follows a particularly simple path whose projection on the plane $y^*=0$ is a straight line, parallel to the ray through the vertex given by $z^*/x^*=w^*$.

The correction $p^*$ to the basic Newtonian pressure only enters the problem through the $y^*$-momentum equation, showing that the pressure arises from centrifugal effects due to streamline curvature in the vertical plane and, of course, the jump conditions at the shock. The pressure may be deduced by direct integration of (2.29) once $v^*$ and $w^*$ are known, and these, in turn, are obtained from (2.27) and (2.30), which may be solved independently of the rest. Solution of these two equations therefore provides the basic problem. The density correction $\sigma^*$ is not required in the determination of $p^*$, so, in this sense, the problem is analogous to one of constant density flow. However, this does not imply that the

flow is in fact at constant density, even to this approximation, since $\sigma^*$ may be evaluated from (2.31) once $u^*$, $v^*$ and $p^*$ are known. The value of $u^*$ is required only if a higher approximation (or $\sigma^*$ of course) is to be calculated. This is straightforward since $u^*$ is constant along a streamline and is therefore given by the value $u_s^*$ just downstream of the shock; determination of $u_s^*$ follows immediately from the solution for the flow field. The Mach angle in the shock layer, as already stated, is proportional to $\epsilon^{\frac{1}{2}} \tan\alpha$ and similarly the shock layer thickness is proportional to $\epsilon \tan\alpha$; on applying the thin shock layer approximation it is found that Mach disturbances propagate immediately from the body to the shock (in the limit $\epsilon \to 0$). This point may be examined in more detail by considering the equations of motion themselves. Equations (2.27)–(2.30) are hyperbolic everywhere, possessing characteristic surfaces across which there may be discontinuities in the derivatives. If these surfaces are defined by

$$f(x^*, y^*, z^*) = \text{constant}$$

then (2.27)–(2.30) may be written in a new characteristic form; it is found that discontinuities in derivatives of $v^*$ and $p^*$ occur wherever

$$\partial f/\partial y^* = 0, \tag{3.2}$$

which is satisfied by surfaces normal to the $x^*, z^*$ plane. Discontinuities in derivatives of $u^*$, $v^*$ and $w^*$ arise when

$$\frac{\partial f}{\partial x^*} + v^* \frac{\partial f}{\partial y^*} + w^* \frac{\partial f}{\partial z^*} = 0. \tag{3.3}$$

This is in fact the equation for a stream surface and expresses the fact that adjacent streamlines may have discontinuities in the derivatives of velocity across them. Returning to the first characteristic surface we note that discontinuities in derivatives of $v^*$ are equivalent to discontinuities in stream surface slope or curvature and that these propagate through the shock layer normal to the plane $x^*$, $z^*$. Typically, therefore, any discontinuity in the curvature of the body surface is equivalent to a discontinuity in surface streamline curvature and will propagate to the shock as above. More specifically, the effect of the singularity in the body and streamline curvature at the sharp leading edge for the detached shock case is also transmitted along the characteristic, so that there is a trace in the shock along which the shock curvature itself must be singular. This trace is then a simple projection of the wing planform. This is an important point which will be used in the discussion of the necessary leading-edge boundary conditions.

## 4. Final formulation of the thin shock layer equations

All the previous work, apart from that of Hillier (1970*b*), was concerned with the conical problem and directly specialized equations (2.27)–(2.30) to this case; the full equations must obviously be used in the study of more general three-dimensional shapes but can be manipulated into a more convenient form. The equations contain $x^*$, $y^*$ and $z^*$ as independent variables and since the main task

of the calculation is to determine the flow field structure and the shock shape it is in fact best now to regard $y^*$ as a dependent variable and to replace it by a new independent variable. It is convenient to take this as the variable denoting a stream surface ($\eta$ = constant say), which is therefore defined by (3.3), i.e.

$$-\left(\frac{\partial y^*}{\partial x^*}\right)_{\eta,z^*}+v^*-w^*\left(\frac{\partial y^*}{\partial z^*}\right)_{\eta,x^*}=0. \tag{4.1}$$

Obviously there is no unique set of stream surfaces; each surface comprises all those streamlines which pass through a particular trace in the flow field or, more conveniently, emanate from a particular trace in the shock. The constant denoting a stream surface in its turn is set by the definition of this trace geometry. The co-ordinate system is modified further still, however. Since the conical problem is an important case, both in its own right and also because the flow at the vertex of the wings is a conical solution, it is useful to employ the conical co-ordinate surfaces $y^*/x^*$ and $z^*/x^*$. The first of these, as already explained, is a dependent variable. The second, together with $\eta$ and $x^*$, provides the three independent variables for the problem. To fully define the notation, therefore, the necessary transformations are given by

$$\left.\begin{aligned} x^*\to x,\quad z^*\to xz,\\ y^*(x^*,\eta,z^*)\to xy(x,\eta,z)\end{aligned}\right\} \tag{4.2}$$

and

$$\left.\begin{aligned} p^*(x^*,y^*,z^*)\to p(x,\eta,z),\\ w^*(x^*,y^*,z^*)\to w(x,\eta,z),\end{aligned}\right\} \tag{4.3}$$

and so on.

The thin shock layer equations (excluding for brevity those for $u^*$ and $\sigma^*$, which are not needed to compute the pressure) now become

$$\frac{\partial y}{\partial\eta}+\frac{\partial w}{\partial z}\frac{\partial y}{\partial\eta}+x\frac{\partial^2 y}{\partial\eta\,\partial x}+(w-z)\frac{\partial^2 y}{\partial\eta\,\partial z}=0, \tag{4.4}$$

$$x\frac{\partial y}{\partial\eta}\frac{\partial v}{\partial x}+(w-z)\frac{\partial y}{\partial\eta}\frac{\partial v}{\partial z}+\frac{\partial p}{\partial\eta}=0, \tag{4.5}$$

$$x\frac{\partial w}{\partial x}+(w-z)\frac{\partial w}{\partial z}=0, \tag{4.6}$$

$$y-v+x\frac{\partial y}{\partial x}+(w-z)\frac{\partial y}{\partial z}=0, \tag{4.7}$$

together with the shock boundary conditions

$$v_s=y_s+x\frac{\partial y_s}{\partial x}+\tau\frac{\partial y_s}{\partial z}-1-\left(\frac{\partial y_s}{\partial z}\right)^2-z\frac{\partial y_s}{\partial z}, \tag{4.8}$$

$$p_s=2y_s+2x\frac{\partial y_s}{\partial x}+2\tau\frac{\partial y_s}{\partial z}-1-\left(\frac{\partial y_s}{\partial z}\right)^2-2z\frac{\partial y_s}{\partial z}, \tag{4.9}$$

$$w_s=\tau-\partial y_s/\partial z. \tag{4.10}$$

Now the body boundary condition is given by (2.32), which is a statement that the body surface is a stream surface. However, (4.1) is also a stream surface

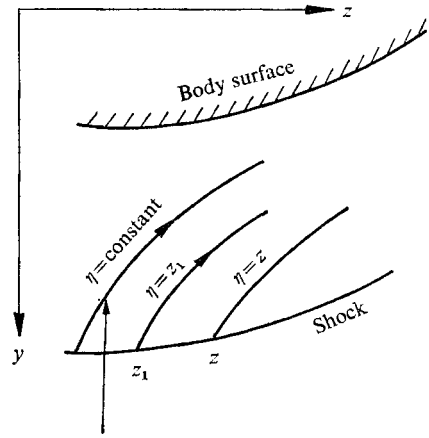


FIGURE 2. Streamline pattern in conical plane.

equation and, when evaluated upon the body, must be identical to (2.32). We therefore obtain

$$\left(\frac{\partial y}{\partial x}\right)_{\text{body}} = \frac{\partial y_B}{\partial x_B}, \quad \left(\frac{\partial y}{\partial z}\right)_{\text{body}} = \frac{\partial y_B}{\partial z_B}. \tag{4.11}$$

## 5. The conical problem

The conical equations of motion are obtained by first defining the stream surface $\eta$ = constant to be a conical surface itself and then equating the derivative $\partial/\partial x$ to zero in the (4.4)–(4.11). It is convenient to consider the flow in the conical cross-plane $(y, z)$. Figure 2 shows a conical streamline traversing the shock layer; this is the projection of the conical stream surface in the $y$, $z$ plane. The sidewash $w$ is constant on this streamline (see § 4), so $w = w(\eta)$ only. There is also an arbitrary constant defining each streamline. Messiter fixed this, for convenience, and without any loss of generality, by putting it equal to the value of $z$ at the point on the shock where the particular streamline commences. With these conical simplifications (4.4) reduces to

$$(w_0(\eta)-z)\left[\frac{\partial}{\partial z}\left(\frac{\partial y_0/\partial \eta}{w_0(\eta)-z}\right)\right] = 0, \tag{5.1}$$

where the subscript 0 denotes conical quantities throughout the remainder of this text. Since $w_0(\eta) \neq z$, in general, (5.1) is integrated twice to give

$$y_0(\eta, z) = \Delta_0 + t_0 + \tau z - \int_0^z w_0(z_1)\, dz_1 + \int_\eta^z \frac{(w_0(\eta_1)-z)}{(w_0(\eta_1)-\eta_1)^2}\, d\eta_1, \tag{5.2}$$

where $\Delta_0$ and $t_0$ are the shock stand-off distance and body thickness, respectively, on the centre-line in the transformed conical plane. Equation (5.2) is now differentiated with respect to $z$ to obtain the streamline slope:

$$\frac{\partial y_0}{\partial z} = \tau - w_0(z) - \frac{1}{w_0(z)-z} + \int_\eta^z \frac{d\eta_1}{(w_0(\eta_1)-\eta_1)^2}. \tag{5.3}$$

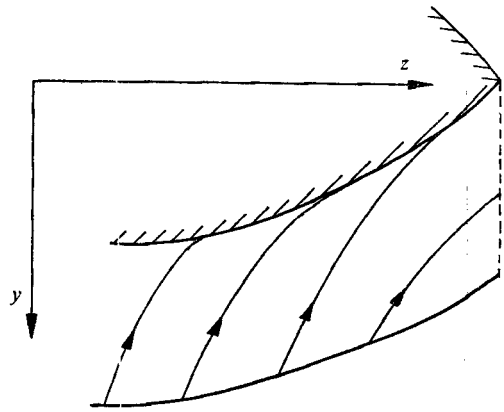


FIGURE 3. Typical streamline pattern in the conical plane for the detached shock case.

Now, the body surface boundary condition (4.11) requires that the streamline slope on the body, $(\partial y_0/\partial z)_{\text{body}}$, should equal the body slope $dy_{0B}/dz_B$. The first of these is simply given by evaluating (5.3) on the body, i.e. at $z = z_B$, which gives

$$\left(\frac{\partial y_0}{\partial z}\right)_{\text{body}} = \tau - w_0(z_B) - \frac{1}{w_0(z_B) - z_B} + \int_{\eta}^{z_B} \frac{d\eta_1}{(w_0(\eta_1) - \eta_1)^2}. \tag{5.4}$$

The body slope, in its turn, is obtained by evaluating (5.2) on the body and then differentiating the resulting equation for $y_{0B}$ with respect to $z_B$. In this differentiation we must make use of the fact that there is a relationship between $z_B$ and $\eta$ on the body, in that every position $z_B$ on the body has a particular streamline $\eta$ associated with it, so that we write

$$z_B = z_B(\eta). \tag{5.5}$$

Using (5.5), the surface slope gives

$$\frac{dy_{0B}}{dz_B} = \tau - w_0(z_B) - \frac{1}{w_0(z_B) - z_B} + \int_{\eta}^{z_B(\eta)} \frac{d\eta_1}{(w_0(\eta_1) - \eta_1)^2} - \frac{(w_0(\eta) - z_B)}{(w_0(\eta) - \eta)^2} \frac{d\eta}{dz_B}. \tag{5.6}$$

Equations (5.4) and (5.6) are then only equivalent if either

$$w_0(\eta) = z_B \tag{5.7a}$$

or

$$d\eta/dz_B = 0. \tag{5.7b}$$

Equations (5.7*a*) and (5.7*b*) constitute the appropriate body surface boundary conditions for the solution of the integral equation (5.6). The first condition (5.7*a*) repeats the statement that any particular streamline may terminate (tangentially) in the conical plane at a spanwise position given by $w_0(\eta) = z_B$; this is taken as the condition for a detached shock and gives flow patterns which are typically like those shown in figure 3. The conical plane gives the appearance of a two-dimensional flow but with some streamlines terminating upon the surface. Obviously this cannot happen in a steady two-dimensional flow, nor in the exact conical solution except at certain singular points. It should be repeated that although some streamlines are terminating in the cross-plane they still possess a component of velocity directed along the wing chord.

For high values of $\Omega$ (i.e. high aspect ratios) the shock wave eventually attaches along the leading edges. The streamline from the leading edge then has a constant sidewash velocity ($w_0 = w_0(\Omega)$ say) and will traverse the cross-plane until it terminates at the position $z_B = w_0(\Omega)$. Such a flow corresponds to the second boundary condition (5.7*b*), which states that $\eta$ may remain constant over part of the body surface. Inboard of the position $z_B = w_0(\Omega)$ the appropriate boundary condition must be reconsidered and it is this particular point which causes some difficulty in the solution of the attached shock problem. There is in fact a minimum value of $\Omega$ below which a shock cannot be attached. This is determined by evaluating (5.6) at the leading edge for an attached shock (where $\eta = z_B = \Omega$). After some manipulation (5.6) reduces to

$$w_0(\pm\Omega) = \frac{1}{2}\left\{\left(\Omega - \left(\frac{dy_{0B}}{dz_B}\right)_{\pm\Omega} + \tau\right) \pm \left[\left(\Omega \pm \left(\frac{dy_{0B}}{dz_B}\right)_{\pm\Omega} \mp \tau\right)^2 - 4\right]^{\frac{1}{2}}\right\}, \tag{5.8}$$

where the upper and lower signs refer to the positive and negative leading edges respectively. Since the sidewash must be real the attached shock equation holds on the positive leading edge provided that

$$\Omega > 2 + \tau - (dy_{0B}/dz_B)_{\Omega} \tag{5.9a}$$

and on the negative side if

$$\Omega > 2 - \tau + (dy_{0B}/dz_B)_{-\Omega}. \tag{5.9b}$$

Equations (5.9*a*) and (5.9*b*) are the leading-edge conditions for an attached shock; various solutions to the appropriate equations have been discussed by Squire (1968*b*), Woods (1970) and Roe (1970, 1971) for wings with flat, diamond and caret cross-sections.

At first sight the thin shock layer equations appear to have lost many features of the full equations of motion (see also Roe 1970), typically in that the former are hyperbolic everywhere whilst the character of the latter depends upon the particular flow region under consideration. However, the thin shock layer equations do reproduce many features of the full equations of motion, as well as providing some excellent comparisons with experiment, and it is particularly useful to consider the velocities in the shock layer *vis-à-vis* whether they are conically supersonic or not. This term, first used by Squire, Jones & Stanbrook (1963), refers to whether the component of fluid velocity normal to a ray through the vertex is supersonic or subsonic. Given that the speed of sound in the shock layer is $\epsilon^{\frac{1}{2}} \sin\alpha \cos\beta \bar{U}_\infty$ it may be shown that the flow is conically supersonic provided that

$$(w_0 - z)^2 > 1, \tag{5.10}$$

$$\left.\begin{aligned} &\text{i.e. either} && (w_0 - z) > 1 \\ &\text{or} && (z - w_0) > 1. \end{aligned}\right\} \tag{5.11}$$

The two conditions determine, respectively, whether there is an outflow (i.e. towards the positive leading edge) or an inflow. To avoid confusion with the phenomena occurring in the exact flow these supersonic and subsonic regions will be referred to in the manner of Hayes & Probstein as supercritical or subcritical.

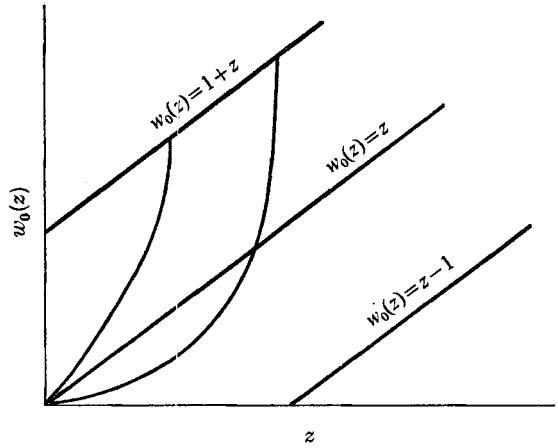


FIGURE 4. Two typical sidewash distributions for the detached shock case showing the singularity at the outwards critical line.

If $\Omega$ falls below the value given by (5.9$a$) or (5.9$b$) then the shock must detach and the flow is subject to the body surface boundary condition (5.7$a$), as already stated. Some consideration must now be given to the necessary leading-edge conditions. It has already been pointed out that the expected effect of the leading-edge singularity in body curvature is to cause a singular trace in the shock, the locus of which is a simple projection of the wing planform. A singularity in shock curvature means, in its turn, a singularity in $dw_0(z)/dz$ at the shock. Differentiation of (5.6) shows that such a singularity occurs when

$$(w_0(z)-z)^2-1=0,$$

i.e. when the flow is critical (see also Messiter and Hayes & Probstein). This bears a close resemblance to the proposed subsonic–supersonic expansion about the leading edge for the real flow, and the appropriate root is therefore taken to give a critical flow outwards. Figure 4 includes two typical plots of $w_0(z)$ for the detached shock case.

The detached shock equations have been solved for a wide variety of cases. These include wings with flat, diamond and caret cross-section (Squire 1966, 1968$a$) and also yawed wings with flat, convex and concave cross-sections (Hillier 1970$a, b$). Furthermore, the last reference also considered cross-sections with slope discontinuities (typically a wing–body configuration) by replacing the discontinuity with a short section of high curvature.

## 6. The simply cambered wing

It was shown in § 3 that the sidewash $w(x, y, z)$ is constant along a streamline. It was also pointed out that a stream surface $\eta$ = constant comprises all those streamlines emanating from a particular trace in the shock surface. It is convenient, furthermore, to assume that in some cases this trace is the locus of all points of constant sidewash (i.e. the locus $\partial y_s/\partial z$ = constant). Therefore we have

that $w(x, y, z) = w(\eta)$ only for this particular case. With this simplification (4.4) and (4.7) reduce to

$$\frac{\partial y}{\partial \eta} + x\frac{\partial^2 y}{\partial \eta\, \partial x} + (w(\eta) - z)\frac{\partial^2 y}{\partial \eta\, \partial z} = 0, \tag{6.1}$$

$$y - v + x\frac{\partial y}{\partial x} + (w(\eta) - z)\frac{\partial y}{\partial z} = 0. \tag{6.2}$$

The first of these, equation (6.1), is rewritten as

$$x\frac{\partial}{\partial x}\left[\frac{\partial y/\partial \eta}{w(\eta) - z}\right] + (w(\eta) - z)\frac{\partial}{\partial z}\left[\frac{\partial y/\partial \eta}{w(\eta) - z}\right] = 0, \tag{6.3}$$

which has the general solution

$$\partial y/\partial \eta = (w(\eta) - z)\, G(\eta)\, H[x(w(\eta) - z)], \tag{6.4}$$

where $G$ and $H$ are two arbitrary functions. When (6.4) is integrated with respect to $\eta$ we obtain the basic stream surface equation:

$$y(x, \eta, z) = y_s(x, z) - \int_{\eta}^{\eta_s(x,z)} G(\eta_1)\, (w(\eta_1) - z)\, H[x(w(\eta_1) - z)]\, d\eta_1, \tag{6.5}$$

where $\eta_s(x, z) =$ constant is the trace in the shock whence a stream surface commences. Now, the body surface boundary conditions were derived in § 4 and require that

$$\left(\frac{\partial y}{\partial z}\right)_{\text{body}} = \frac{\partial y_B}{\partial z_B}, \quad \left(\frac{\partial y}{\partial x}\right)_{\text{body}} = \frac{\partial y_B}{\partial x_B} \quad \text{on} \quad y = y_B. \tag{6.6}$$

The general streamline slope in the cross-plane, $\partial y/\partial z$, is obtained by differentiating (6.5) with respect to $z$ and is given by

$$\frac{\partial y}{\partial z} = \frac{\partial y_s}{\partial z} - \frac{\partial \eta_s}{\partial z} G(\eta_s)\, (w(\eta_s) - z)\, H[x(w(\eta_s) - z)] - \int_{\eta}^{\eta_s(x,z)} G(\eta_1)\frac{\partial}{\partial z}\{(w(\eta_1) - z)\, H[x(w(\eta_1) - z)]\}\, d\eta_1, \tag{6.7}$$

whilst the corresponding component of slope in the $x$ direction is

$$\frac{\partial y}{\partial x} = \frac{\partial y_s}{\partial x} - \frac{\partial \eta_s}{\partial x} G(\eta_s)\, (w(\eta_s) - z)\, H[x(w(\eta_s) - z)] - \int_{\eta}^{\eta_s(x,z)} G(\eta_1)\, (w(\eta_1) - z)\frac{\partial}{\partial x}\{H[x(w(\eta_1) - z)]\}\, d\eta_1. \tag{6.8}$$

The values for the components of stream surface slope on the body are then given simply by replacing $x$ and $z$ by $x_B$ and $z_B$ in (6.7) and (6.8). The body slopes in these two directions are obtained by substituting $x_B$ and $z_B$ respectively into (6.5) to give the equation for the body shape $y_B$, and then differentiating this with respect to $x_B$ or $z_B$. This gives

$$\frac{\partial y_B}{\partial x_B} = \frac{\partial y_s}{\partial x_B} - \int_{\eta}^{\eta_s} G(\eta_1)\, (w(\eta_1) - z_B)\frac{\partial}{\partial x_B}\{H[x_B(w(\eta_1) - z_B)]\}\, d\eta_1 - \frac{\partial \eta_s}{\partial x_B} G(\eta_s)\, (w(\eta_s) - x_B)\, H[x_B(w(\eta_s) - z_B)] + \frac{\partial \eta}{\partial x_B} G(\eta)\, (w(\eta) - z_B)\, H[x_B(w(\eta) - z_B)] \tag{6.9}$$

and
$$\frac{\partial y_B}{\partial z_B} = \frac{\partial y_s}{\partial z_B} - \int_{\eta}^{\eta_s} G(\eta_1) \frac{\partial}{\partial z_B} \{(w(\eta_1) - z_B) H[x_B(w(\eta_1) - z_B)]\} d\eta_1$$
$$- \frac{\partial \eta_s}{\partial z_B} G(\eta_s) (w(\eta_s) - z_B) H[x_B(w(\eta_s) - z_B)]$$
$$+ \frac{\partial \eta}{\partial z_B} G(\eta) (w(\eta) - z_B) H[x_B(w(\eta) - z)]. \qquad (6.10)$$

If (6.7) is now equated with (6.9), and (6.8) with (6.10), in order to satisfy the condition (6.6) we must have either

$$\frac{\partial \eta}{\partial x_B} = \frac{\partial \eta}{\partial z_B} = 0 \qquad (6.11a)$$

or
$$w(\eta) = z_B. \qquad (6.11b)$$

We again note that (6.11*a*) implies that the stream surface may lie coincident with the body surface for some distance and that this corresponds to the attached shock case. The second equation (6.11*b*) repeats that streamline paths eventually become asymptotic to the plane $z$ = constant, and again this is taken as the detached shock condition.

The arbitrary functions of integration $G$ and $H$ are determined by equating the values of $v$ at the shock as determined both from the shock boundary condition (4.8) and also from the appropriate equation of motion (6.2). These are equal only if

$$1 = (w(\eta_s) - z) \left\{ x \frac{\partial \eta_s}{\partial x} + (w(\eta_s) - z) \frac{\partial \eta_s}{\partial z} \right\} G(\eta_s) H[x(w(\eta_s) - z)]. \qquad (6.12)$$

So far the analysis has been perfectly general and no geometrical limitations have been placed upon the body shape. Evaluation of $G$ and $H$ from (6.12) is a complicated task, other than for the simplest forms for $\eta_s(x, z)$, so that it is best to make some assumptions as to its form. The easiest case is that when $\eta_s(x, z) = z$, which includes all conical flows; it also, more generally, covers all those cases where the wing planform is itself conical. This is because by setting $\eta_s(x, z) = z$ we are also stating that the sidewash at the shock is then a function of $z$ only which, in its turn, means that profiles of the transverse shock slope $\partial y_s/\partial z$ are self-similar for all values of $x$. This, therefore, places strict limitations upon any trace of curvature discontinuity in the shock. First, there may be a discontinuity along the line $x$ = constant since this will not defy the requirements on the self-similarity of the transverse slope. This particular case corresponds to curvature discontinuities in the chordwise camber of the wing and will not be considered further here. The second possibility is that the trace lies along the line $z$ = constant. Thus the discontinuity in shock curvature due to the wing leading edge can only lie along such a line, which implies, from § 3, that the wing planform is itself conical.

Then, with the assumption that $\eta_s(x, z) = z$, equation (6.12) gives

$$1 = (w(z) - z)^2 G(z) H[x(w(z) - z)]. \qquad (6.13)$$

This shows that $H[x(w(z)-z)]$ is constant ($=H$, say) and that

$$G(z) = 1/H \times (w(z)-z)^2. \tag{6.14}$$

The basic stream surface equation (6.5) for this particular flow then reduces to

$$y(x,\eta,z) = y_s(x,z) - \int_\eta^z \frac{(w(\eta_1)-z)}{(w(\eta_1)-\eta_1)^2}\,d\eta_1. \tag{6.15}$$

The shock shape $y_s(x,z)$ is evaluated in terms of the sidewash at the shock, $w_s(x,z) = w_s(z)$, by using the boundary condition (4.10). Thus

$$y_s(x,z) = \Delta(x) + t(x) + \tau z - \int_0^z w(z_1)\,dz_1, \tag{6.16}$$

where $\Delta(x)$ and $t(x)$ are the shock stand-off distance and body thickness, respectively, along the centre-line in this transformed plane.

The two governing equations (6.9) and (6.10) now become

$$\frac{\partial y_B}{\partial x_B} = \frac{d}{dx_B}[\Delta(x_B) + t(x_B)] \tag{6.17}$$

and

$$\frac{\partial y_B}{\partial z_B} = \tau - w(z_B) - \frac{1}{w(z_B)-z_B} + \int_{\eta(z_B)}^{z_B} \frac{d\eta_1}{(w(\eta_1)-\eta_1)^2}. \tag{6.18}$$

Equation (6.17) shows that $\partial y_B/\partial x_B$ is a function of $x_B$ only, so that the body shape is of the simple three-dimensional form

$$y_B(x_B, z_B) = y_{0B}(z_B) + y_B^*(x_B). \tag{6.19}$$

Equation (6.19) defines what is termed as the simply cambered wing since it possesses a basic conical distribution of thickness, $y_{0B}(z_B)$, superimposed upon a surface, $y_B^*(x_B)$, cambered in the chordwise direction. The sidewash distribution for this wing is given by the solution of (6.18) and depends only upon the conical component of geometry $y_{0B}(z_B)$, so that we can replace $w(\eta)$ by $w_0(\eta)$, the equivalent conical result. The thickness of the shock layer $y_s(x,z) - y_B(x_B, z_B)$ is obtained by evaluating (6.15) on the body. This is again simply the conical result, so that we have $y_s(x,z) - y_B(x_B,z_B) = y_{0s}(z) - y_{0B}(z_B)$ and $\Delta(x) = \Delta_0$. After some algebra the pressure equation (4.5) can be integrated to give

$$p_B(x_B, z_B) = p_{0B}(z_B) + 2y_B^*(x_B) + 2x_B\frac{dy_B^*}{dx_B} + x_B(y_{0s} - y_{0B})\left(\frac{2dy_B^*}{dx_B} + x_B\frac{d^2y_B^*}{dx_B^2}\right), \tag{6.20}$$

that is, the basic conical term $p_{0B}(z_B)$ plus a relatively simple correction in terms of $x_B$.

The preceding results all demonstrate various important features of the simply cambered wing. The flow field structure is essentially determined by the conical geometry at the vertex, so that, within this approximation, whether the shock attaches along the whole line of the leading edge or not depends only upon whether the conditions (5.9*a*) and (5.9*b*) are satisfied. Pressure distributions may be obtained for any of the conical shapes from the quoted references. The three-dimensional correction to the basic conical pressure in (6.20) depends only upon

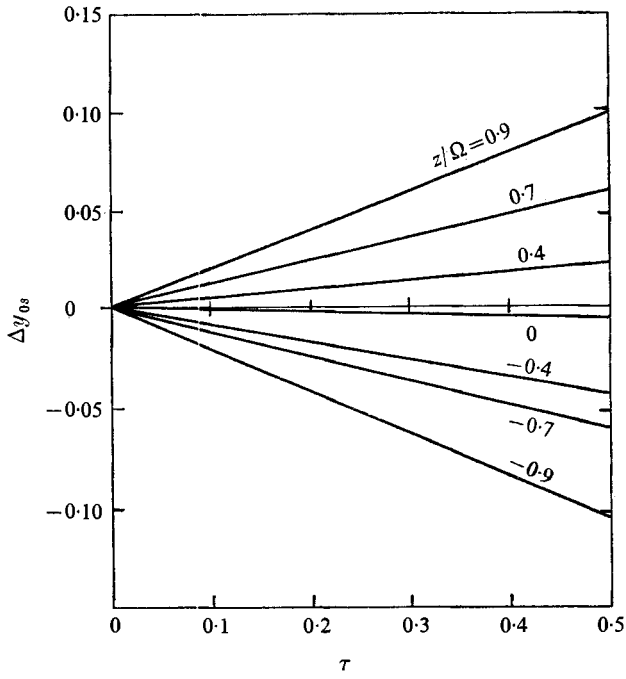


FIGURE 5. Perturbation in the conical shock shape due to yaw.

the local body geometry as opposed to the conical term itself, which is an integral over the cross-plane. Furthermore, the effects of cambering such a wing can be seen quite clearly and may be of use in optimizing the shape. It has been shown (Hillier 1970*b*) that the effect of yawing a conical wing is to decrease $y_{0s}-y_{0B}$ on the side of negative $z_B$ and to increase it on the other; this holds for a wide variety of cross-sections and the appropriate perturbation in shock shape from the unyawed value is given in figure 5. There is then a coupling between yaw and camber such that, typically, for the case $d^2y_B/dz_B^2 \equiv 0$ the induced rolling moment due to camber is stabilizing provided that $dy_B/dz_B$ is negative.

## 7. Perturbation solution for more general wings

The analysis of the previous section was exact, within the context of thin shock layer theory, up to (6.12), where a particular form was then assumed for the trace $\eta_s(x,z)$ = constant in the shock along which the sidewash was constant. In general it is not possible to postulate the required form of $\eta_s(x,z)$ *a priori*, so that it becomes difficult to evaluate the functions $G$ and $H$; for these more complicated problems a different approach has been used. The first departure from the method of the previous section is again to define a stream surface as emanating from a particular trace in the shock but, in this case, to remove the restriction that this be a line of constant sidewash. Since each wing has a sharp vertex the flow, in the limit $x \to 0$, corresponds to a conical result which will be assumed already known. It is then convenient to consider the flow over the rest of the

body as a perturbation of this conical flow, the dependence on $x$ being expressed explicitly by taking $x$ as the perturbation parameter. This greatly simplifies the analysis required and also facilitates the tabulation of the final results. The flow properties therefore become functions of two variables only ($\eta$ and $z$). It is best still to retain $\eta$ as an independent variable but in some cases, for example, the non-conical planform, the surfaces $z$ = constant may not be the natural co-ordinate surfaces for the problem. Let us consider the case where the body differs slightly from a conical wing both in the thickness distribution and also in the planform geometry. This shape can be written as

$$y_B(x_B, z_B) = y_{0B}(r_B) + \sum_1^\infty x^i y_{iB}(r_B), \tag{7.1}$$

where $r_B$ is a variable representing a straining upon the $z_B$ co-ordinate and is itself given by

$$z_B = r_B + \sum_1^\infty x^i z_{iB}(r_B). \tag{7.2}$$

The trace $r_B = \Omega$ defines the leading edge, the value of $\Omega$ being given by the conical geometry at the wing vertex (i.e. $\Omega = \cot\theta/\epsilon^{\frac{1}{2}}\tan\alpha$). It is reasonable to assume a similar straining throughout the flow field and to express $z$ as

$$z = r + \sum_1^\infty x^i z_i(r, \eta), \tag{7.3}$$

where $r$ is now employed as the independent variable instead of $z$, and $z_i(r, \eta)$ evaluated upon the body is the $z_{iB}$ of (7.2). We now set the constant on the trace $\eta_s(x, z)$ by writing $\eta_s(x, z) = r$. Thus, although an individual streamline is still a trajectory of constant sidewash $w$ the stream surface $\eta$ = constant, composed of all the streamlines originating at $\eta_s(x, z) = r$, is not necessarily a surface of constant $w$.

In order to be consistent with the expansions (7.1) and (7.3) the flow variables in the shock layer are written as

$$\left.\begin{aligned} y(x, \eta, z) &= y_0(r, \eta) + \sum_1^\infty x^i y_i(r, \eta), \\ w(x, \eta, z) &= w_0(r, \eta) + \sum_1^\infty x^i w_i(r, \eta), \\ v(x, \eta, z) &= v_0(r, \eta) + \sum_1^\infty x^i v_i(r, \eta), \\ p(x, \eta, z) &= p_0(r, \eta) + \sum_1^\infty x^i p_i(r, \eta), \end{aligned}\right\} \tag{7.4}$$

where the subscript 0 refers to the basic conical solution at the vertex, corresponding to the conical body geometry term $y_{0B}(r_B)$, and the other terms constitute higher order corrections to this result. When the expansions (7.4) are substituted into the thin shock layer equations (4.4)–(4.11) and the coefficients of the $x^i$ are identically equated to zero, a set of approximate equations results for each correction, i.e. value of $i$. The form of the expansions (7.4) points out certain

features of this particular method even before we present these equations. The conical terms form the same conical equations as those given in § 5 except that $r$ now replaces $z$; thus discontinuities in streamline curvature must now propagate along the surface $r$ = constant. This is only compatible with the original discussion of § 3 if the surface $r$ = constant lies normal to the plane $(x, z)$, i.e. if $z_i(r, \eta) = z_i(r)$ only or if $z_i(r) = z_{iB}(r_B)$. This is assumed henceforth. When deriving the corrections in powers of $x$ it is only necessary to demonstrate the first one ($i = 1$) since the manipulations for the higher corrections, although more complicated algebraically, are precisely similar in principle. The equations for the first correction are

$$(w_0(\eta)-r)^3\frac{\partial}{\partial r}\left\{\frac{(\partial y_1/\partial\eta)}{(w_0(\eta)-r)^2}\right\}+\frac{\partial}{\partial r}\left(w_1\frac{\partial y_0}{\partial\eta}\right) - \frac{\partial^2 y_0}{\partial\eta\,\partial r}(w_0(\eta)-r)^3\frac{\partial}{\partial r}\left\{\frac{z_1}{(w_0(\eta)-r)}\right\}=0, \tag{7.5}$$

$$-\left(\frac{\partial v_0}{\partial r}\frac{\partial y_0}{\partial\eta}\right)(w_0(\eta)-r)^3\frac{\partial}{\partial r}\left\{\frac{z_1}{(w_0(\eta)-r)^2}\right\}+v_1+v_1\frac{\partial y_1}{\partial\eta} + (w_0(\eta)-r)\left(\frac{\partial v_0}{\partial r}\frac{\partial y_1}{\partial\eta}\right)+(w_0(\eta)-r)\left(\frac{\partial y_0}{\partial r}\frac{\partial v_1}{\partial r}\right)+\frac{\partial p_1}{\partial\eta}=0, \tag{7.6}$$

$$w_1+(w_0(\eta)-r)\,\partial w_1/\partial r=0, \tag{7.7}$$

$$2y_1-v_1-2z_1\frac{\partial y_0}{\partial r}+(w_0(\eta)-r)\left(\frac{\partial y_1}{\partial r}-\frac{\partial z_1}{\partial r}\frac{\partial y_0}{\partial r}\right)=0, \tag{7.8}$$

together with the shock boundary conditions

$$v_{1s}=2y_{1s}-\frac{dy_{0s}}{dr}\left(2z_1-r\frac{dz_1}{dr}\right)-r\frac{dy_{1s}}{dr}-2w_{0s}w_{1s}, \tag{7.9}$$

$$p_{1s}=4y_{1s}-2\frac{dy_{0s}}{dr}\left(2z_1-r\frac{dz_1}{dr}\right)-2r\frac{dy_{1s}}{dr}-2w_{0s}w_{1s}, \tag{7.10}$$

$$w_{1s}=\frac{dz_1}{dr}\frac{dy_{0s}}{dr}-\frac{dy_{1s}}{dr} \tag{7.11}$$

and the body surface tangency condition

$$\left(\frac{\partial y_1}{\partial r}\right)_{\text{body}}=\frac{dy_{1B}}{dr_B}\quad\text{on}\quad y_1=y_{1B}. \tag{7.12}$$

Equation (7.7) integrates to give the basic sidewash relation

$$w_1(r,\eta)=A_1(\eta)\,(w_0(\eta)-r), \tag{7.13}$$

where $A_1(\eta)$ is an arbitrary function, introduced by the integration, which is treated as the unknown. Equation (7.5) is integrated twice to give

$$y_1(r,\eta)-z_1(r)\frac{\partial y_0}{\partial r}=G_2(r)-2\int_\eta^r A_1(\eta_1)\frac{(w_0(\eta_1)-r)}{(w_0(\eta_1)-\eta_1)^2}\,d\eta_1 - \int_\eta^r G_1(\eta_1)\,(w_0(\eta_1)-r)^2\,d\eta_1, \tag{7.14}$$

where $G_1(\eta)$ and $G_2(r)$ are two further functions of integration. It is unnecessary to evaluate these yet and an important point is raised if the body boundary condition (7.12) is now considered. The technique of equating the surface streamline slope to the body slope has been discussed in § 6, so it is only necessary to present the resulting condition here; this gives

$$2\frac{A_1(\eta)\,(w_0(\eta)-r_B)}{(w_0(\eta)-\eta)^2}\frac{d\eta}{dr_B}+G_1(\eta)\,(w_0(\eta)-r_B)^2\frac{d\eta}{dr_B}-\frac{z_{1B}}{(w_0(\eta)-\eta)^2}\frac{d\eta}{dr_B}=0. \quad (7.15)$$

Since $G_1(\eta)$ is finite the first two terms of (7.15) are independently zero as a result of the form of the basic conical solution. However, the last term of (7.15) is zero only if either

$$\left.\begin{aligned} z_{1B} &= 0,\\ \text{or}\qquad d\eta/dr_B &= 0.\end{aligned}\right\} \quad (7.16)$$

If the detached shock boundary condition holds in the basic conical problem (i.e. $w_0(\eta) = r_B$) then $d\eta/dr_B$ is not zero in general and we must therefore apply the condition $z_{1B} = 0$ from (7.16). This means that there can be no straining of the planform in the detached shock case and that, therefore, the detached solution only applies to wings with delta planforms. When the attached shock conditions hold in the basic conical problem, however, we have that $d\eta/dr_B = 0$, so that, from (7.16), there may be finite values of $z_{1B}$. Thus we may obtain solutions for the flow in the vicinity of a curved leading edge with an attached shock wave. For the remainder of the analysis we shall consider only the case $z_{1B} = 0$, i.e. the delta planform. With $z_{1B} = 0$ the streamline equation (7.14) reduces to

$$y_1(r,\eta) = y_{1s}(r)-2\int_\eta^r A_1(\eta_1)\frac{(w_0(\eta_1)-r)}{(w_0(\eta_1)-\eta_1)^2}\,d\eta_1-\int_\eta^r G_1(\eta_1)\,(w_0(\eta_1)-r)^2\,d\eta_1, \quad (7.17)$$

where the two functions of integration, $y_{1s}(r)$ and $G_1(\eta)$, are determined by considering the appropriate shock boundary conditions. Equation (7.11) shows that

$$y_{1s}(r) = \Delta_1+t_1-\int_0^r A_1(r_1)\,(w_0(r_1)-r_1)\,dr_1, \quad (7.18)$$

where $\Delta_1$ and $t_1$ are the first corrections to the conical solution for the shock stand-off distance and body thickness, respectively, on the centre-line. $G_1(\eta)$ is itself determined by equating the values of $v_1$ at the shock as given by the equation of motion (7.8) and by the shock boundary condition (7.9); the result shows that

$$G_1(\eta) = -3A_1(\eta)/(w_0(\eta)-\eta)^2. \quad (7.19)$$

Equations (7.18) and (7.19) are incorporated into the expression for $dy_{1B}/dr_B$ to give the governing equation:

$$\frac{dy_{1B}}{dr_B} = -A_1(r_B)\,(w_0(r_B)-r_B)+\frac{A_1(r_B)}{w_0(r_B)-r_B} +2\int_\eta^{r_B}\frac{A_1(\eta_1)\,(3r_B-2w_0(\eta_1)-\eta_1)}{(w_0(\eta_1)-\eta_1)^3}\,d\eta_1. \quad (7.20)$$

Once the function $A_1(\eta)$ is known, $p_{1B}(r_B)$ can be obtained by integrating (7.6) subject to the shock condition (7.10). This is written, after considerable algebra, in a form amenable to numerical integration, so that

$$\begin{aligned} p_{1B} &= 2(\Delta_1+t_1)(2+y_{0s}-y_{0B})-2A_1(r_B)(w_0(r_B)-r_B)^2 \\ &\quad -2(2+y_{0s}-y_{0B})\int_0^{r_B} A_1(r_1)(w_0(r_1)-r_1)\,dr_1 \\ &\quad +\int_\eta^{r_B}\left\{X_1(r_B,\eta_1)+\frac{(w_0(\eta_1)-r_B)}{(w_0(\eta_1)-\eta_1)^2}\int_{\eta_1}^{r_B} X_2(\eta_1,t)\,dt\right\}d\eta_1 \qquad (7.21) \\ &= 2(\Delta_1+t_1)(2+y_{0s}-y_{0B})+p^*_{1B}(r_B) \quad \text{(say)}, \qquad (7.22) \end{aligned}$$

where $X_1(r,\eta_1)$ and $X_2(\eta_1,t)$ are two complicated functions given in appendix A. It should be noted that (7.22) also holds for the yawed wing although the appropriate parameter $\tau$ does not appear explicitly. To evaluate (7.22) completely we need to know $\Delta_1$. This can be shown to be zero for the unyawed wing and obtained as a simple function of $A_1(z)$ for the yawed case. This derivation is shown in appendix B as it is not of immediate importance here.

## 8. Some simple solutions to the integral equation (7.21)

Despite the complexity of any general solution there are several comparatively simple results. The previous section showed that $\Delta_1 = 0$ for the unyawed wing which indicates that near the centre-line the shock profile is dominated by the conical terms. Not surprisingly, the centre-line pressure can be written with corresponding simplicity. Since $A_1(t)$ must be of order $t$ for $t\to 0$ (from equation (7.20)) and, similarly, since the conical sidewash term $w_0(t)$ must be of order $t$ (from equation (5.3)), inspection of (7.21) shows that $p^*_{1B}(r_B)$ must also be of order $r_B$ near the centre-line, so that

$$p^*_{1B}(0) = 0. \qquad (8.1)$$

The centre-line pressure correction on the unyawed wing then becomes

$$p_{1B}(0) = 2t_1(2+\Delta_0). \qquad (8.2)$$

Although the simply cambered wing was discussed earlier it should be noted that by setting $dy_{1B}/dr_B \equiv 0$ we get $A_1(\eta) \equiv 0$, which gives in its turn

$$\left.\begin{aligned} y_{1s}-y_{1B} &\equiv 0, \\ p_{1B} &= 2t_1(2+y_{0s}-y_{0B}). \end{aligned}\right\} \qquad (8.3)$$

These equations are the same as those for the more general case of § 6.

Another simple case concerns the conditions at the leading edge when the shock is attached. Considering only the unyawed case, for simplicity, equation (7.20) gives at the leading edge (where $\eta = r_B = \Omega$)

$$\left(\frac{dy_{1B}}{dr_B}\right)_\Omega = -A_1(\Omega)(w_0(\Omega)-\Omega)+\frac{A_1(\Omega)}{w_0(\Omega)-\Omega}. \qquad (8.4)$$

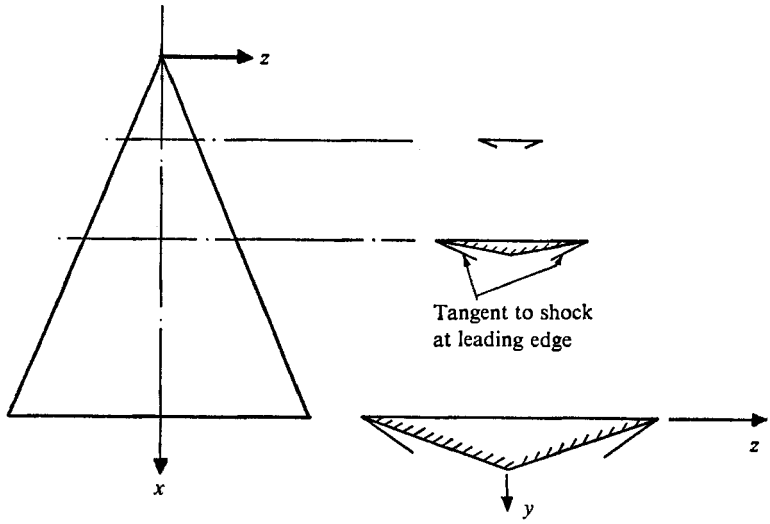


FIGURE 6. Simple three-dimensional wing with the shock attached at the leading edge.

Since $w_1(\Omega) = A_1(\Omega)\,(w_0(\Omega) - \Omega)$ we obtain

$$w_1(\Omega) = \left(\frac{dy_{1B}}{dr_B}\right) \frac{(w_0(\Omega) - \Omega)^2}{[1 - (w_0(\Omega) - \Omega)^2]}, \tag{8.5}$$

and the surface pressure at the leading edge is determined from (7.21). Noting first that

$$y_{1s} - y_{1B} = \Delta_1 + t_1 - \int_0^r A_1(r_1)\,(A_1(r_1) - r_1)\,dr_1 \tag{8.6}$$

and that this is obviously zero at the leading edge for an attached shock, the appropriate pressure term is

$$p_{1B}(\Omega) = 4y_{1B}(\Omega) - 2w_1(\Omega)\,(w_0(\Omega) - \Omega). \tag{8.7}$$

The value of $w_0(\Omega)$ itself is given by the attachment conditions for the conical problem as was explained previously in § 5. Equation (8.7) constitutes a useful check upon the theory since it may be compared with the pressure given by the exact oblique shock relations. Typically, for the configuration† shown in figure 6, equation (8.7) predicts that for a one degree change in dihedral angle, measured normal to the leading edge, the pressure coefficient changes by $+0{\cdot}0043$. This compares favourably with the exact value of $+0{\cdot}0049$.

## 9. Numerical solution of (7.20)

Generally the equation must be solved numerically, because of the complicated nature of the functions involved. A numerical solution for the detached shock case has been proposed by the author (Hillier 1970*b*); since it is essentially a standard procedure for integral equations there is no need to repeat many details

† Assuming an incidence of 8° at $M_\infty = 10$ for a 70° swept delta.

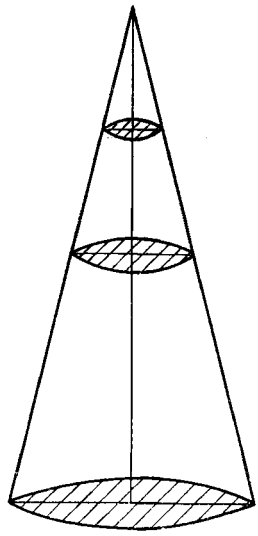

FIGURE 7. Lens section wing showing typical section shapes.

here. Numerical integration is not possible near the origin, because of the singular nature of the terms involved, and the solution is given in this vicinity by a power series of the form (B 2) see (appendix B). Sufficiently far from the origin the integration is continued numerically, marching in small steps until the leading edge is reached. Generally a step size of about 0·001 is needed; this is the same as for the computations carried out for the conical case by Squire and Hillier.

As yet the numerical calculation has been applied to one case only. This is the lens section wing, typically of the form shown in figure 7, where the shape is given in the physical plane by

$$\bar{y}_B/\bar{x} = h\left(1-\frac{\bar{z}^2}{b^2\bar{x}^2}\right)(1-\kappa\bar{x}/\bar{c}) \tag{9.1}$$

and in the transformed plane by

$$y_B = t_0(1-r^2/\Omega^2)(1-\kappa x). \tag{9.2}$$

The basic conical wing for this problem is the convex section case computed by the author and which has already been extensively tabulated. The most convenient way to express the surface pressure $p_{0B}(r_B)$ on such wings is to present it as a function of the reduced sweepback parameter $\Omega$ and also a reduced thickness parameter† $c/\Omega$.

The first correction to the pressure $p_{1B}$ is likewise a function of $c/\Omega$ and $\Omega$ and so far results have only been computed for the particular case $c/\Omega = 0{\cdot}55$. The distribution of $p_{1B}$ over the wing span at $\Omega = 0{\cdot}91$ is shown in figure 8; the particular values of these two parameters correspond to the conditions of an experimental comparison which will be discussed later in § 11. There is a singularity in $p_{1B}$ (strictly in $p^*_{1B}$) at the leading edge, this singularity being connected

† The thickness parameter $c = h/b\epsilon^{\frac{1}{2}} = t_0/\Omega$, first used by Squire (1966) and Hida (1965), is a measure of the wing thickness in the transformed plane.

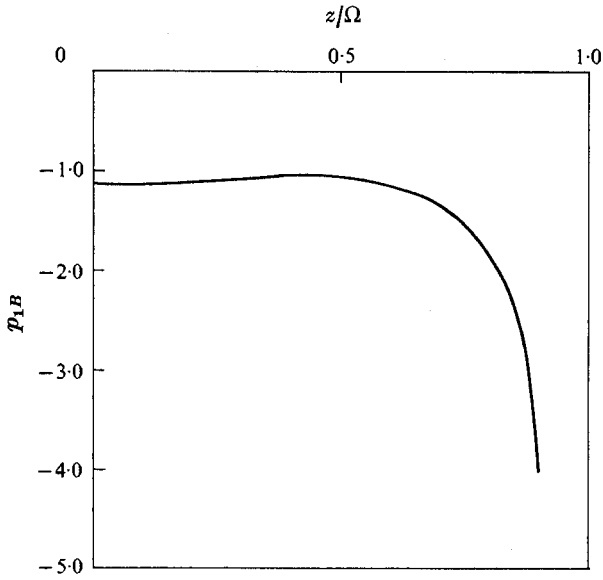


FIGURE 8. Distribution of $p_{1B}$ across span of lens section wing ($\Omega = 0{\cdot}91$, $C/\Omega = 0{\cdot}55$).

with the critical flow of the basic conical solution although no detailed investigation has been made as to its behaviour. Thus the expansions (7.4) are not valid everywhere; most obviously they fail rapidly at the leading edge. Unfortunately the radius of convergence of these series can only be assessed by calculating higher order terms, which is in itself a complicated task. Therefore no practical limitation may be put upon $xp_{1B}$, or more probably $xp^*_{1B}$. However, it would be realistic to assume that the approximation cannot hold for values of $xp^*_{1B}$ much greater than unity.

It is possible that such a numerical approach may also hold for the attached shock problem. However, no attempt has been made to evaluate this case, which is likely to possess additional difficulties, as exemplified by the essentially discontinuous solution for the basic conical problem (see Squire, Woods & Roe).

## 10. Higher corrections for three-dimensional wings

The perturbation technique has been demonstrated in the previous sections; it requires only increased algebraic and numerical complexity to evaluate the higher order terms. Although no general results have been derived it in fact becomes obvious that each sidewash component $w_i(r, \eta)$ will be characterized by an arbitrary function $A_i(\eta)$ (say), which will, in turn, be related to the appropriate perturbation in the body shape by an integral equation. The algebra for the second correction has been performed by Hillier (1970*b*) and that for the next is by no means prohibitive although an explicit formulation for the pressure integral in terms of $A_i(\eta)$ is likely to prove so. However, the $y$-momentum equation could be integrated numerically, without the intermediate algebraic manipulations, although this would require a considerably larger computer store.

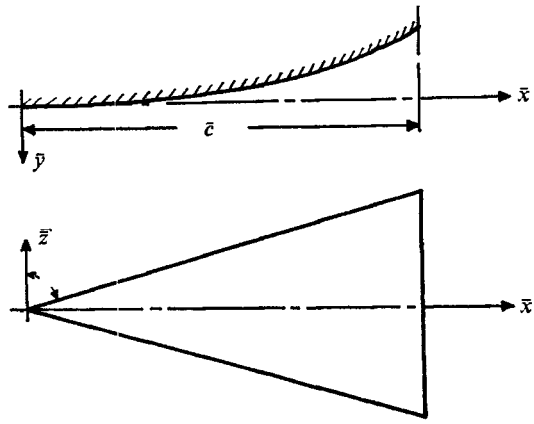


FIGURE 9. Geometry of the simply cambered wings ($\bar{c}$ = 90·5 mm for −4·6° camber; $\bar{c}$ = 90·0 mm for −10·3° camber).

The simply cambered case has already been solved in § 6; it is possible, however, to derive the result inductively via the perturbation method and the relevant analysis is shown by Hillier (1970*b*). A further important result may also be proved by an inductive process; this relates to the conditions on the centre-line of any unyawed wing of conical planform and gives

$$\Delta_i = 0, \quad p_{iB} = 2(i+1)\,t_i(1+\tfrac{1}{2}i\Delta_0),$$

where $t_i$ is the $i$th correction to the body thickness on the centre-line. Since the relevant analysis has not been presented elsewhere it is reproduced in appendix C for completeness.

## 11. Comparisons of thin shock layer theory with experiment

In all the quoted references on conical flows there were a considerable number of comparisons made between theory and experiment which, almost without exception, showed excellent agreement. This was particularly encouraging since these results covered geometries with a wide variety of cross-sections, conditions of both attached and detached shocks as well as the influence of yaw, and also values of the incident Mach number and angle of incidence which could hardly be considered hypersonic. Indeed, the initial requirement of the theory was that the parameter $\epsilon$ be small compared with unity and yet there are many instances where there is in fact excellent agreement for values of order unity (see for example Squire 1968*a*, *b*; Hillier 1970*a*, *b*). The reason for this is unknown but in the checks upon the three-dimensional theory comparisons have again been made for shapes differing considerably from the original requirement of a nearly plane surface as well as for large values of $\epsilon$.

The first case compared with experiment is for the simply cambered wing since this does not contain the truncation errors inherent in the perturbation approach. There are two sets of results available, both of which were obtained by the author (Hillier 1970*b*, 1971) in the supersonic wind tunnels of the Cambridge University Engineering Department. The wing was originally a flat delta, with sweep angle

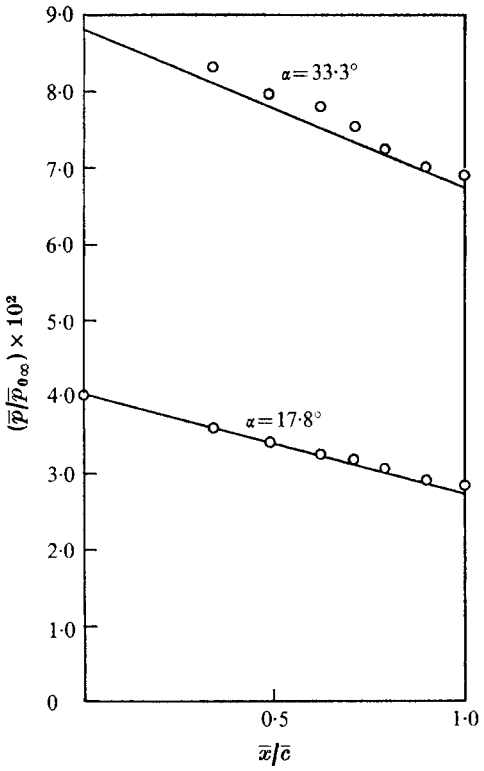


FIGURE 10

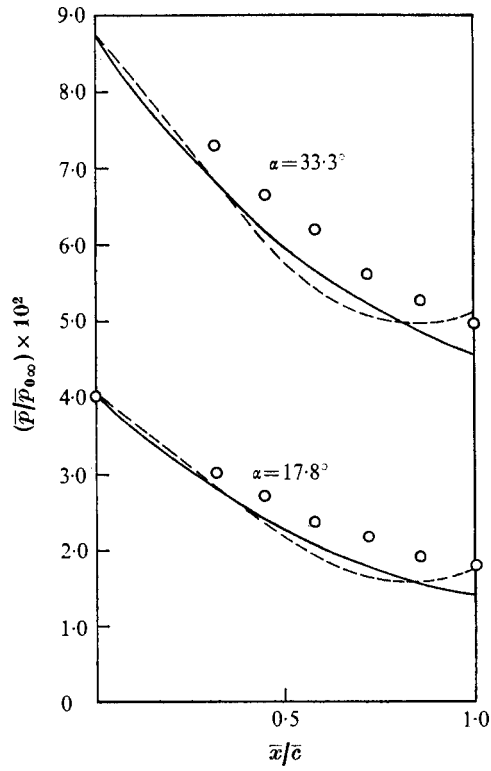


FIGURE 11

FIGURE 10. Comparison between theory and experiment for the $-4{\cdot}6°$ cambered wing ($M_\infty = 3{\cdot}51$, $\bar{p}_{0\infty}$ = free-stream stagnation pressure). O, experiment; ——, theory. For $\alpha = 33{\cdot}3°$, $\epsilon = 0{\cdot}392$, $\Omega = 0{\cdot}674$; for $\alpha = 17{\cdot}8°$, $\epsilon = 0{\cdot}890$, $\Omega = 0{\cdot}913$.

FIGURE 11. Comparison between theory and experiment for the $-10{\cdot}3°$ cambered wing ($M_\infty = 3{\cdot}51$). ——, two-term theory; – – –, three-term theory. For $\alpha = 33{\cdot}3°$, $\epsilon = 0{\cdot}392$, $\Omega = 0{\cdot}674$; for $\alpha = 17{\cdot}8°$, $\epsilon = 0{\cdot}890$, $\Omega = 0{\cdot}913$.

$\theta = 74{\cdot}55°$, which had then been bent in the chordwise direction. For the first case the resulting angle was $-4{\cdot}6°$ and in the second case it was $-10{\cdot}3°$; the camber angle is defined in this case as the change in body slope from the vertex to the unit chord position. The geometry is more clearly defined in figure 9. The shape of the first wing, in physical co-ordinates, can be closely approximated by the equation

$$\bar{y}_B(\bar{x}, \bar{z})/\bar{x} = -0{\cdot}0402(\bar{x}/\bar{c}).$$

There was some difficulty in precisely defining the body shape for the second case, as explained in the references, and two closely matching forms have been suggested. These are

$$\bar{y}_B(\bar{x}, \bar{z})/\bar{x} = -0{\cdot}1350(\bar{x}/\bar{c}) + 0{\cdot}0295(\bar{x}/\bar{c})^2$$

and

$$\bar{y}_B(\bar{x}, \bar{z})/\bar{x} = -0{\cdot}1027(\bar{x}/\bar{c}) - 0{\cdot}0480(\bar{x}/\bar{c})^2 + 0{\cdot}0420(\bar{x}/\bar{c})^3.$$

Figures 10 and 11 compare the theoretical and experimental pressure distributions along the centre-lines of the two wings when unyawed. Both give good

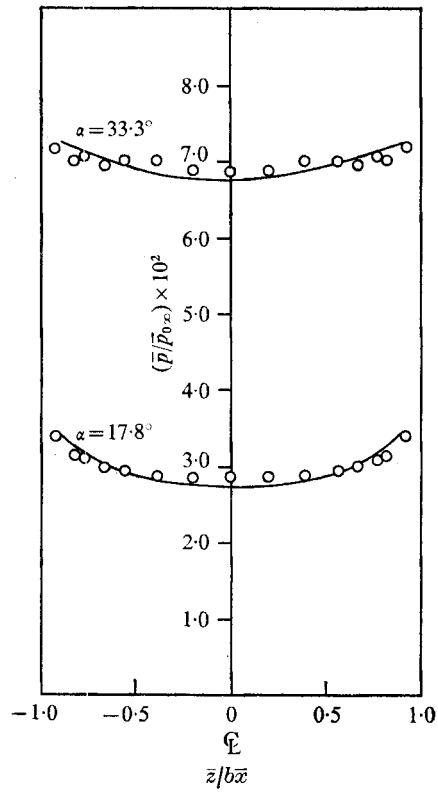


FIGURE 12. Comparison between theory and experiment for the $-4{\cdot}6°$ cambered wing ($M_\infty = 3{\cdot}51$, $\bar{x}/\bar{c} = 1{\cdot}0$).

agreement although the predicted results tend to be low for the wing with $-10{\cdot}3°$ camber. This may partially reflect the fact that the planform is no longer strictly delta but, having been bent, is of the form

$$\bar{z}/\bar{x} = b + O(x^2).$$

No allowance has been made for this in the comparisons shown. Further effects are due to the low incidence of the trailing edge, which is only $7{\cdot}5°$ for the lowest incidence tests, so that the flow is not strictly hypersonic there, and also because, at these low incidences, the model is no longer completely immersed in the accurately calibrated region of supersonic flow and is subjected to Mach number gradients of uncertain magnitude. The three-term series predicts a slight recompression at the rear of the wing whilst the two-term series shows no such trend. This discrepancy reflects a failure of the power series representation for large values of $\bar{x}/\bar{c}$ and demonstrates the need for a more refined method of model construction if the more detailed points of the pressure distributions are to be investigated.

Figure 12 shows the spanwise pressure distributions at the rear of the $4{\cdot}6°$ cambered wing whilst figures 13 and 14 show the corresponding distributions on the $10{\cdot}3°$ cambered wing for both the unyawed and yawed cases. The particular

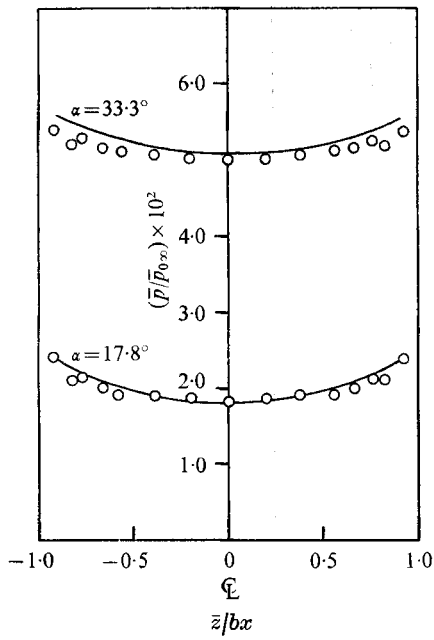


FIGURE 13

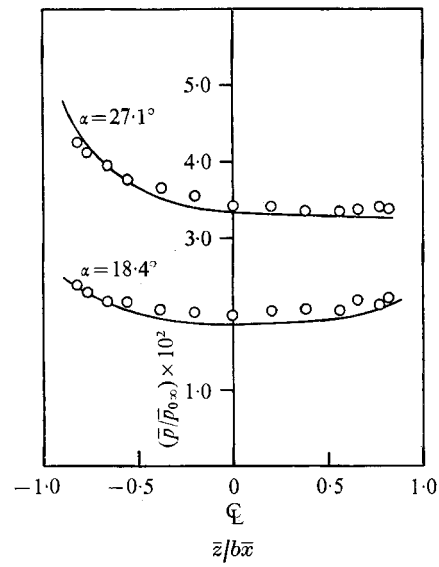


FIGURE 14

FIGURE 13. Comparison between theory and experiment for the −10·3° cambered wing ($M_\infty = 3{\cdot}51$, $\bar{x}/\bar{c} = 1{\cdot}0$).

FIGURE 14. Comparison between theory and experiment for the yawed wing (−10·3° camber, $M_\infty = 3{\cdot}51$, $\bar{x}/\bar{c} = 1{\cdot}0$). For $\alpha = 27{\cdot}1°$, $\beta = 4{\cdot}95°$, $\epsilon = 0{\cdot}48$, $\tau = 0{\cdot}27$; for $\alpha = 18{\cdot}4°$, $\beta = 1{\cdot}45°$, $\epsilon = 0{\cdot}84$, $\tau = 0{\cdot}09$.

body shape used for this second wing is the three-term series; use of the two-term series does not affect the shape of the curve but only the overall pressure level. In all cases agreement between theory and experiment is close.

The second experimental comparison concerns a wing with delta planform and diamond cross-section tested at a Mach number of 3·97 by the Royal Aircraft Establishment at Bedford (Moore, private communication). The wing has a polynomial distribution of thickness and is described in the physical plane by

$$\frac{\bar{y}_B}{\bar{x}} = h\left\{1 - 2{\cdot}5\frac{\bar{x}}{\bar{c}} + 2{\cdot}5\left(\frac{\bar{x}}{\bar{c}}\right)^2 - 1{\cdot}25\left(\frac{\bar{x}}{\bar{c}}\right)^3 + 0{\cdot}25\left(\frac{\bar{x}}{\bar{c}}\right)^4\right\}\left(1 - \frac{\bar{z}}{b\bar{x}}\right),$$

where $h = 0{\cdot}315$ and $b = 0{\cdot}333$.

Figure 15 compares the theoretical and experimental pressure distributions along the centre-line at an incidence of 22°. Agreement is good over the first 25 % of the chord, where a large percentage of the pressure drop occurs, and then the theory tends to overpredict the fall in pressure. No experimental points are included for the rear 40 % of the chord since these were effected by the model support. There are several factors to be considered when studying the theoretical result: first, there is a slight disagreement at the vertex and this basic error is reproduced along the centre-line. This discrepancy at the apex is a result of use of the conical theory and arises because the model cross-section is very thick. Indeed

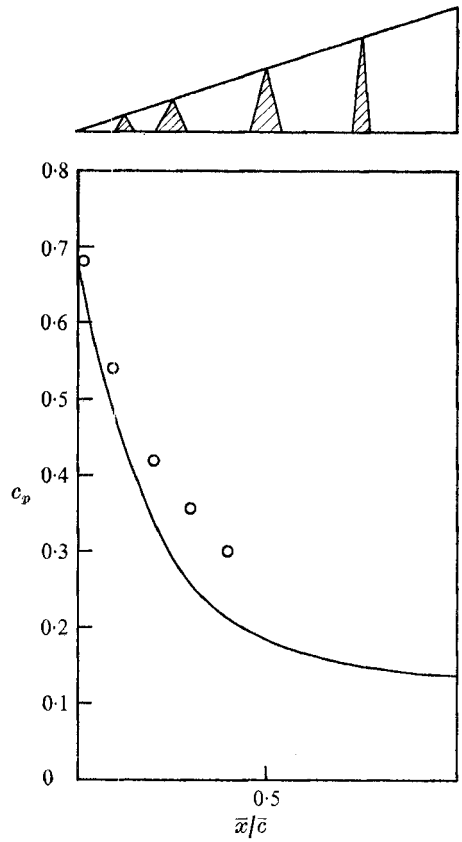


FIGURE 15. Pressure distribution along wing centre-line (typical wing sections also shown). $M_\infty = 3{\cdot}97$, $\alpha = 22°$.

the thickness parameter $c$ ($= h/be^{\frac{1}{2}}$) is 1·28, which is in itself a severe test of the conical theory since it represents a considerable departure from a plane body. Not only is the body very thick, however, but there is a large camber along the centre-line which curves 20·2° from the vertex to the 40 % chord position and 39° over the whole chord.

The third important comparison is for a wing tested at a Mach number of 4·0 by Larcombe (private communication) at the National Physical Laboratory. The wing is of the 'lens' section type described in (9.1) and in this case $\kappa = 0{\cdot}5$, $h = 0{\cdot}105$ and $b = 0{\cdot}25$. The wing was tested at an incidence of 18°, to give $\Omega = 0{\cdot}91$ and $c/\Omega = 0{\cdot}55$; the corresponding distribution of $p_{1B}$ across the span has already been discussed in § 9 and tabulated in figure 8.

Figure 16 compares the theory and experiment for this case. The computed centre-line pressure, as has already been explained in § 10, is exact within thin shock layer theory since the centre-line is a path of constant curvature. This implies a linear variation of pressure from the vertex and such a prediction is reasonably justified by the results. Off the centre-line the solution is no longer exact but contains truncation errors of uncertain magnitude, together with the

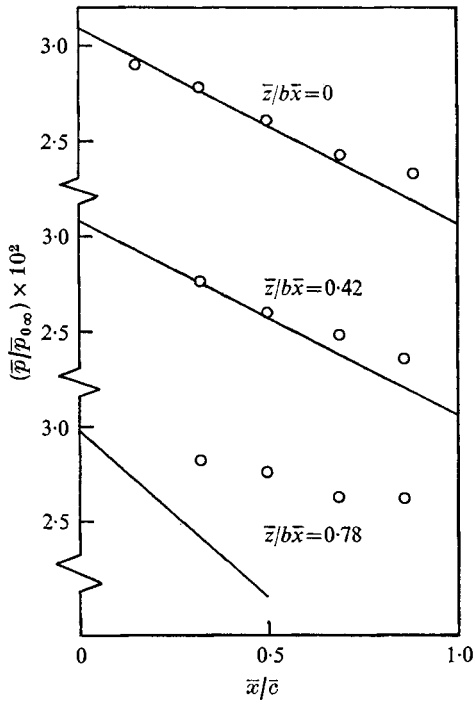


FIGURE 16. Comparison between theory and experiment for the lens section wing ($M_\infty = 4{\cdot}0$, $\alpha = 18°$).

failure of the theory near the leading edge. Certainly agreement is good along the ray $\bar{z}/b\bar{x} = 0{\cdot}42$, where $p^*_{1B}$ is still small, but there is a large error along

$$\bar{z}/b\bar{x} = 0{\cdot}78,$$

which is within the region of influence of the leading edge.

## 12. Conclusions

Thin shock layer theory has now been applied to a wide variety of problems in several papers. The conical case is particularly well documented and there is probably a more comprehensive range of results for such wings using this theory than for any other single approach.

This paper shows some useful extensions of the technique to non-conical wings. The simply cambered case is clearcut, giving an exact solution, of particularly simple form, which agrees well with experiment. Although further experimental checking is obviously required this case is likely to prove an important result, especially in view of the large range of section geometries to which it is applicable.

It seems unlikely that an exact solution, or more precisely a final integral equation, will be derived for the more complicated three-dimensional geometries and this paper has resorted to the assumption that the flow field is a perturbation upon a known conical flow. Again this exhibits some simple features in that the centre-line shock stand-off distance varies linearly from the vertex, irrespective

of the actual geometry, and the centre-line pressure is a simple function of this stand-off distance.

The benefit of a perturbation approach is that it facilitates the tabulation of results as well as simplifying the governing equations. This does not imply, however, that it is the only useful technique, or even the best, and there may be some advantages, in fact, in a direct numerical solution of (4.3)–(4.11), based upon a known conical flow field for $x = 0$, although such an approach has not yet been investigated.

Another point which has received little attention in the development of this particular wing theory is the validity of the thin shock layer expansions near the body surface. The conical problem exemplifies this in that streamlines terminate upon the surface in the cross-plane, whilst still satisfying the tangency condition, although such behaviour is only true at particular singular points of the real flow. This results from the absence of a lateral pressure gradient term in the $z$-momentum equation; near the body surface, where the cross-flow velocity term is itself small, the pressure gradient is no longer insignificant and should strictly be retained. The requirement then is not just a single expansion throughout the flow field but an outer and inner expansion instead, matched, perhaps, by a third intermediate zone. Hayes & Probstein, as well as Roe (1970), have indicated approaches to this, whilst Melnik & Scheuing (1962) have considered a more general conical case. The essential point shown by these analyses, however, is that the surface pressure is still given correctly to order $\epsilon$, so that we do not need to resort to a more complicated approach to calculate this. It is reasonable to assume that similar results hold in this three-dimensional analysis and that the main (initial) tests of this assumption should be by experimental comparisons.

During the period of this research the author was in receipt of a grant from the Science Research Council. He would also like to express his gratitude to Dr L. C. Squire for many helpful discussions.

## Appendix A

The two functions $X_1$ and $X_2$ in the pressure equation (7.22) are given respectively by

$$X_1(\eta_1, r_B) = A_1(\eta_1)\frac{(w_0(\eta_1)-r_B)^3}{(w_0(\eta_1)-\eta_1)^2}\,w_0'(r_B)\left\{-1+\frac{1}{(w_0(r_B)-r_B)^2}\right\}\left\{1+3\,\frac{(r_B-\eta_1)}{(w_0(\eta_1)-\eta_1)}\right\}$$
$$+\frac{A_1(r_B)\,(w_0(\eta_1)-r_B)^2}{(w_0(r_B)-r_B)^3\,(w_0(\eta_1)-\eta_1)^2}\{4r_B w_0(\eta_1)-4w_0(\eta_1)\,w_0(r_B)+2(w_0^2(r_B)-r_B^2)\}$$
$$-\frac{A_1(r_B)\,(w_0(\eta_1)-r_B)^2}{(w_0(\eta_1)-\eta_1)^2}\left\{2(w_0(r_B)-r_B)+(w_0(\eta_1)-r_B)\,(w_0'(r_B)-r_B)\right.$$
$$\left.\times\left[1+\frac{1}{(w_0(r_B)-r_B)^2}\right]\right\}$$
$$+\frac{A_1'(r_B)\,(w_0(\eta_1)-r_B)^3}{(w_0(\eta_1)-\eta_1)^2}\left\{\frac{1}{(w_0(r_B)-r_B)}-(w_0(r_B)-r_B)\right\},$$

$$X_2(\eta_1, t) = \frac{A_1(t)}{(w_0(t)-t)^3}\{-8w_0(\eta_1)\,w_0(t)-4tw_0(\eta_1)+4tw_0(t)+2w_0^2(t)+6w_0^2(\eta_1)\},$$

where the prime denotes differentiation.

## Appendix B. The determination of $\Delta_1$ for the detached shock case

If we consider a yawed wing, for which the basic conical solution is known, then the trace of $w_0(t)$ between the two leading edges must cross the line $w_0(t) = t$ at least once. This is a line of zero conical cross-flow and if we denote this particular value of $t$ by $\zeta_0$, it can be shown (see Hillier 1970*a*, *b*) that $w_0(t)$ may be written as a series expansion about $\zeta_0$ of the form

$$w_0(t) - \zeta_0 = \sum_1^\infty a_i (t-\zeta_0)^i, \tag{B 1}$$

for which the first few coefficients $a_i$ have been calculated by Squire (1966) and Hillier (1970*a*, *b*).

The function $A_1(t)$ can be written as a similar series about $\zeta_0$:

$$A_1(t) = \sum^\infty \alpha_i (t-\zeta_0)^i, \tag{B 2}$$

where the individual $\alpha_i$ are obtained by substituting the series into the integral equation (7.20) and then equating coefficients of $(t-\zeta_0)^i$. This gives $\alpha_0 = 0$; if (7.17) is now evaluated on the body (at $r_B = \zeta_0$) we obtain

$$y_{1s}(\zeta_0) - y_{1B}(\zeta_0) = O(r_B - \zeta_0), \tag{B 3}$$

which is of course zero. If the wing is unyawed then $\Delta_1$ automatically becomes zero. If the wing is yawed the value $\Delta_1$ is given simply from (7.18) by

$$\Delta_1 + t_1 = y_{1B}(\zeta_0) + \int_0^{\zeta_0} A_1(r_1)\,(w_0(r_1) - r_1)\,dr_1. \tag{B 4}$$

## Appendix C. General term for the centre-line pressure correction

To calculate this general ($i$th) correction we need to assess the orders of magnitude of the flow variables, and their derivatives, in all the preceding lower order corrections. These are obviously unknown, except in specific cases, and it is necessary to make certain assumptions as to their form which will then be justified *a posteriori*. Assume then that near the wing centre-line (i.e. as $z, \eta \to 0$) the solution is known for the $j$*th* correction (where $1 \leqslant j < i$) and more specifically that

$$w_j(z,\eta) = O(q^2), \tag{C 1}$$

$$y_j(z,\eta) = t_j + O(q), \tag{C 2}$$

where $t_j$ is the $j$th correction to the body thickness upon the centre-line in the transformed plane and the expression $O(q)$ implies terms of the order $\eta, z, z^2/\eta$, etc. Noting, furthermore, that $w_0(\eta) = O(\eta)$ we may evaluate (4.6) for the $i$th correction to give

$$i w_i + (w_0(\eta) - z)\frac{\partial w_i}{\partial z} = -\sum_{j=1}^{i-1} w_j \frac{\partial w_{i-j}}{\partial z}, \tag{C 3}$$

or

$$w_i = A_i(\eta)\,(w_0(\eta) - z)^i + O(q^3). \tag{C 4}$$

The streamline structure is determined by using (4.4) for the $i$th term, which shows that

$$(w_0(\eta)-z)^{i+2}\frac{\partial}{\partial z}\left\{\frac{(\partial y_i/\partial\eta)}{(w_0(\eta)-z)^{i+1}}\right\}+\frac{\partial}{\partial z}\left\{w_i\frac{\partial y_0}{\partial\eta}\right\}=-\sum_{j=1}^{i-1}\left\{\frac{\partial w_j}{\partial z}\frac{\partial y_{i-j}}{\partial\eta}+w_j\frac{\partial^2 y_{i-j}}{\partial\eta\,\partial z}\right\}$$
$$=O(q). \tag{C 5}$$

Then,
$$\frac{\partial}{\partial z}\left\{\frac{(\partial y_i/\partial\eta)}{(w_0(\eta)-z)^{i+1}}\right\}-\frac{(i+1)A_i(\eta)}{(w_0(\eta)-z)^2(w_0(\eta)-\eta)^2}=O(q^{-i-1}), \tag{C 6}$$

which gives on integration

$$y_i(z,\eta)=y_{is}(z)-\int_\eta^z G_i(\eta_1)(w_0(\eta_1)-z)^{i+1}\,d\eta_1$$
$$-(i+1)\int_\eta^z\frac{A_i(\eta_1)(w_0(\eta_1)-z)^i}{(w_0(\eta_1)-\eta_1)^2}\,d\eta_1+O(q^2). \tag{C 7}$$

The shock boundary condition (4.10) expresses $y_{is}(z)$ in terms of $A_i(z)$ as

$$y_{is}(z)=\Delta_i+t_i-\int_0^z A_i(z_1)(w_0(z_1)-z_1)^i\,dz_1+O(q) \tag{C 8}$$

and $G_i(\eta)$ may be rewritten, as before, by considering the values of $v_i$ at the shock as given both by the shock boundary condition (4.8) and also by the equation of motion (4.7). After some algebra these show that

$$G_i(\eta)=-(i+2)A_i(\eta)/(w_0(\eta)-\eta)^3+O(q^{-i}). \tag{C 9}$$

Thus the full equation for the streamline shape is

$$y_i(z,\eta)=\Delta_i+t_i-\int_0^z A_i(z_1)(w_0(z_1)-z_1)^i\,dz_1+(i+2)\int_\eta^z A_i(\eta_1)\frac{(w_0(\eta_1)-z)^{i+1}}{(w_0(\eta_1)-\eta_1)^3}\,d\eta_1$$
$$-(i+1)\int_\eta^z\frac{A_i(\eta_1)(w_0(\eta_1)-z)^i}{(w_0(\eta_1)-\eta_1)^2}\,d\eta_1+O(q^2). \tag{C 10}$$

The behaviour of $A_i(\eta)$ itself near the centre-line may be determined by evaluating (C 10) on the body (i.e. $z=z_B$) to give the equation for the body shape $y_{iB}$:

$$y_{iB}(z_B)=\Delta_i+t_i-\int_0^{z_B}A_i(z_1)(w_0(z_1)-z_1)^i\,dz_1$$
$$+(i+2)\int_{\eta(z_B)}^{z_B}A_i(\eta_1)\frac{(w_0(\eta_1)-z_B)^{i+1}}{(w_0(\eta_1)-\eta_1)^3}\,d\eta_1$$
$$-(i+1)\int_{\eta(z_B)}^{z_B}A_i(\eta_1)\frac{(w_0(\eta_1)-z_B)^i}{(w_0(\eta_1)-\eta_1)}\,d\eta_1+O(z_B^2). \tag{C 11}$$

Differentiating (C 11) with respect to $z_B$ gives the local body slope near the origin which is known to be of order unity, so that, in its turn, $A_i(\eta)=O(\eta^{-i+2})$. By reverting again to the equation for $y_{iB}$ it can now be seen that $\Delta_i$ must in fact be zero. These latter results show that both $w_i$ and $y_i$ conform with the original assumptions (C 1) and (C 2); since these assumptions are known to hold for the first correction as given in § 5 all the preceding order-of-magnitude arguments

indeed hold for the general correction terms near the centre-line. It should be noted that the integrals of (C 10) also include terms of the form $z \log z/\eta$, but that these are themselves of order $z$. It is now a matter simply of algebraic manipulation to calculate the centre-line pressure from (4.5) and (4.9), which give

$$p_{iB}(0) = 2(i+1)\, t_i(1 + \tfrac{1}{2} i \Delta_0). \tag{C 12}$$

## REFERENCES


ANTONOV, A. M. & HAYES, W. D. 1966 Calculation of the hypersonic flow about blunt bodies. *J. Appl. Math. Mech.* **30**, 421–427.

COLE, J. D. & BRAINERD, J. J. 1962 Slender wings at high angles of attack in hypersonic flows. In *Hypersonic Flow Research* (ed. F. R. Riddell), pp. 321–343. Academic.

HAYES, W. D. & PROBSTEIN, R. F. 1966 *Hypersonic Flow Theory. Part* 1. *Inviscid Flows.* Academic.

HIDA, K. 1965 Thickness effects on the force of slender delta wings in hypersonic flow. *A.I.A.A. J.* **3**, 427–433.

HILLIER, R. 1970*a* The effects of yaw on conical wings at high supersonic speeds. *Aero. Quart.* **21**, 199–210.

HILLIER, R. 1970*b* Some applications of thin shock layer theory to hypersonic wings. Ph.D. dissertation, University of Cambridge.

HILLIER, R. 1971 Pressure distributions at $M_\infty = 3{\cdot}51$ and at high incidences on four wings with delta planform. *Aero. Res. Counc. Current Paper,* no. 1198.

MELNIK, R. E. & SCHEUING, R. A. 1962 Shock layer structure and entropy layers in hypersonic conical flows. In *Hypersonic Flow Research* (ed. F. R. Riddell), pp. 379–420. Academic.

MESSITER, A. F. 1963 Lift of slender delta wings according to Newtonian theory. *A.I.A.A. J.* **1**, 794–802.

ROE, P. L. 1970 Aerodynamic problems of hypersonic aircraft. Von Kármán Institute short course.

ROE, P. L. 1971 A simple treatment of the attached shock layer on a delta wing. *R.A.E.* unpublished work.

SQUIRE, J. C. 1966 Calculated pressure distributions and shock shapes on thick conical wings at high supersonic speeds. *Aero. Quart.* **18**, 185–206.

SQUIRE, L. C. 1968*a* Calculation of pressure distributions on lifting conical wings with application to the off design behaviour of wave riders. *AGARD Conf. Proc.* p. 30.

SQUIRE, L. C. 1968*b* Calculated pressure distributions and shock shapes on conical wings with attached shock waves. *Aero. Quart.* **19**, 31–50.

SQUIRE, L. C., JONES, J. G. & STANBROOK, A. 1963 An experimental investigation of the characteristics of some plane and cambered 65° delta wings at Mach numbers from 0·7 to 2·0. *Aero. Res. Counc. R. & M.* no. 3305.

WOODS, B. A. 1970 Hypersonic flow with attached shock waves over delta wings. *Aero. Quart.* **21**, 379–399.